Arabian Journal of Chemistry (2023) **16**, 104968

King Saud University

Arabian Journal of Chemistry

www.ksu.edu.sa
www.sciencedirect.com

ORIGINAL ARTICLE

Honokiol attenuates ductular reaction, regulates of bile acids metabolism, and inhibits inflammatory response in murine cholestatic liver injury model

Juan Hao [a,b], Xiaoyu Shen [a], Xiaohong Shao [a], Chunling Zhu [a], Kan Lu [a], Yi Xu [a], Yiyue Chen [a], Jibo Liu [a], Yaqin Ding [a,c], Xin Xie [a], Jian Wu [a,b,*], Quanjun Yang [d,*]

[a] *Department of Endocrinology, Shanghai TCM-Integrated Hospital Affiliated to Shanghai University of Traditional Chinese Medicine, Shanghai, China*
[b] *Shanghai University of Traditional Chinese Medicine, Shanghai, China*
[c] *Medical Office, Shanghai TCM-Integrated Hospital Affiliated to Shanghai University of Traditional Chinese Medicine, Shanghai, China*
[d] *Department of Pharmacy, Shanghai Sixth People Hospital affiliated Shanghai Jiao Tong University School of Medicine, Shanghai, China*

Received 20 June 2022; accepted 27 April 2023
Available online 4 May 2023

KEYWORDS

Honokiol;
Cholestasis;
Bile acids;
Inflammatory;
Fibrosis

Abstract Chronic cholestasis liver injury occurs in progressive hepatobiliary diseases that eventually lead to end-stage liver problems without curable treatment. Great advances in the molecular mechanism suggest the therapeutic pathways for the regulation of bile acid (BA) metabolism and inflammation response. Honokiol (HNK) is a natural ingredient from herb Magnolia officinalis that is used for eliminating toxins, reducing stagnation, resolving stasis and enhancing body immunity. In the present study, we designed two dependent experiments for the evaluation of the hepatoprotective and hepatotoxicity effects of HNK. Chronic cholestasis liver injury model was established by 0.1% 3,5-diethoxycarbonyl-1,4-dihydrocollidine (DDC) containing diet feed for 4 weeks that featured as a ductular reaction, BAs accumulation, fibrosis and inflammatory response. In the first experiment, two dosages of HNK (2 and 10 mg/kg) were daily intraperitoneal injected from day 15 to day 28 for the treatment of chronic cholestasis liver injury. HNK displayed a dosage-dependent reduction of ductular reaction, regulation of BAs metabolism, remission of

* Corresponding authors at: Yishan 600, Xuhui, Shanghai 200233, China(Q. Yang), Baoding 230, Hongkou, Shanghai, 200233, China(J. Wu).
E-mail addresses: haojuan111111@163.com (J. Hao), shenxiaoyu1986@126.com (X. Shen), shaoxiaohongsh@163.com (X. Shao), zhuchunling007@163.com (C. Zhu), mouse_1985@126.com (K. Lu), yi.xu.tcm@outlook.com (Y. Xu), 13636398956@163.com (Y. Chen), liujibo2005@163.com (J. Liu), yaqinding@163.com (Y. Ding), xiexin0929@126.com (X. Xie), 13661561759@126.com (J. Wu), 7250003599@shsmu.edu.cn (Q. Yang).
Peer review under responsibility of King Saud University.

Production and hosting by Elsevier

https://doi.org/10.1016/j.arabjc.2023.104968

fibrosis and inhibition of inflammatory response. In the second experiment, the high dosage of HNK (10 mg/kg) was daily intraperitoneal injected into normal control and model mice for 4 weeks. HNK-mediated hepatoprotective effect is mainly involved in the regulation of BAs metabolism, decrease of inflammatory cell infiltration and inhibition of pro-inflammatory cytokines production. Moreover, HNK showed no hepatotoxicity even though the high dosage of HNK treatment for 28 days in control mice resulted in no obvious change in hepatic histopathological and serological changes. In conclusion, HNK exerts dosage-dependent pharmacological effect against DDC diet-induced chronic cholestasis liver injury. Further investigation of the preclinical pharmacodynamics effect and toxicity research about HNK is helpful for active therapeutic drug development for the treatment of cholestasis liver disease.

1. Introduction

Chronic cholestasis liver injury occurs in diseases such as biliary atresia, primary biliary cirrhosis, and primary sclerosing cholangitis, and causes progressive hepatobiliary diseases that eventually lead to end-stage liver disease(Woolbright and Jaeschke 2012, Ibrahim et al., 2022). This disease is characterized by dysfunction of hepatocytes or obstruction of bile ducts, resulting in the accumulation of toxic bile acid (BA) and infiltrating immune cells in the liver(Woolbright 2020, Cai and Boyer 2021). To date, the pathogenesis of chronic cholestasis liver injury remains ambiguous, and the treatment options are limited (Pablo Arab et al., 2017). Great advances in the molecular mechanism of BAs and immune system interaction suggest the therapeutic pathways for the regulation of BAs metabolism and inflammation response.

Complementary and alternative treatments of chronic cholestasis liver injury have been under active research worldwide(Ma et al., 2020). In Chinese medicine, chronic cholestasis liver injury was thought to be caused by 'poor blood circulation, toxin stagnation and a deficiency of healthy energy' (YueCheng and ChengWei 2019). Thus many herbs from Chinese medicines have been investigated for eliminating toxins, reducing stagnation, resolving stasis and enhancing body immunity(Yang et al., 2018, Wang et al., 2020, Shi et al., 2021, Shi et al., 2022). Clinically, *Magnolia officinalis* is commonly used in TCM formulation for the protection against liver injury (Yin et al., 2009, Seo et al., 2014). In our preliminary experiment, we found Honokiol (HNK) alleviated cholestatic liver injury and fibrosis. HNK is a natural compound contained in the herb *Magnolia officinalis*(Rajgopal et al., 2016). HNK including formulations shows beneficial effects on inhibition of fatty liver and hepatic lipogenesis since it ameliorated high fat diet - induced hepatic steatosis and liver dysfunction(Lee et al., 2015). HNK protects hepatocytes from apoptosis induced by glycochenodeoxycholic acid in vitro and this protection may be due to reduced oxidative stress (Park et al., 2006). HNK eliminates BA–induced oxidative stress response in malignant and nonmalignant epithelial cells (Chen et al., 2009). HNK alleviates acetaminophen overdose induced liver injury through regulated inhibition of CYP2E1 and CYP2A1 as well as enhancing the generation of GSH (Yu et al., 2019). CYP2Ea and CYP2A1 were enzymes that induced by cocktail incubation and were associated with liver injury. Moreover, HNK showed immune and metabolism regulation potential (Kim and Cho 2008, Lee and Cho 2009, Kim et al., 2013, Seo et al., 2015, Jeong et al., 2016, Jiraviriyakul et al., 2019). Those evidences indicated HNK has the potential for hepatoprotective effect against cholestasis liver injury.

In the present study, we used 3,5-diethoxycarbonyl-1,4-dihydrocol lidine (DDC) induced cholestasis liver injury model to evaluate the comprehensive hepatoprotective and hepatotoxicity effect of HNK. DDC diet induced cholestasis liver injury showed cholestasis related clinical features such as dysfunction of hepatocytes, obstruction of bile ducts, accumulation of BAs and infiltration of immunocytes in the liver(Mariotti et al., 2019, Pose et al., 2019, Li et al., 2021). This model is appropriate for the study of the molecular mechanism and treatment strategy(Fickert et al., 2007, Jemail et al., 2018, Wen et al., 2021). In the present study, we designed two dependent experiments of in vivo murine model for the evaluation of HNK mediated effect on cholestasis liver injury.

2. Materials and methods

2.1. Materials

HNK was purchased from Selleck (Shanghai, China). DDC was purchased from Sigma–Aldrich (St. Louis, USA). Control diets (grain-based rodent diet, 4.5% fat) and control diets supplemented with 0.1% DDC were both purchased from Trophic Animal Feed High-Tech Co. Ltd (Jiangsu, China). BAs, including ursodeoxycholic-2,2,4,4-d4 acid (UDCA-D4, 904171), and lithocholic 2,2,4,4-d4(LCA-D4, 589349), cholic acid (CA, C1129), α-Muricholic acid (α-MCA, 700232P), β-muricholic acid (β-MCA, SML2372), chenodeoxy cholic acid (CDCA, C9377), glycocholic acid (GCA, G2878), taurocholic acid (TCA, T4009), tauro-α-muricholic acid (T-α-MCA, 700243P), tauro-β-muricholic acid (T-β-MCA, 700244P), tauro-chenodeoxycholic acid (TCDCA, T6260), deoxycholicacid (DCA, D2510), ursodeoxycholic acid (UDCA, U5127), lithocholic acid (LCA, L6250), ω-muricholic acid (ω-MCA, 700231P), taurodeoxycholic acid (TDCA, T0875), tauroursodeoxycholic acid (TUDCA, T0266), taurolithocholic acid (TLCA, T7515), tauro-ω-muricholic acid (T-ω-MCA, 700245P) were purchased from Sigma–Aldrich (St. Louis, USA). All other chemicals were obtained from commercial sources.

2.2. Chronic cholestasis liver injury model

The male mice were purchased from the Shanghai Sipple Bikai Laboratory Animal Co., Ltd (Shanghai, China). All mice were kept under specific pathogen free conditions in Shanghai University of Traditional Chinese Medicine (Shanghai, China). After all mice were adapted to the normal diet and drinking for one week, set up a normal diet control group and DDC diet experimental group. The DDC model mice were fed with 0.1% DDC for 4 weeks and it mainly caused bile duct injury and intrahepatic cholestasis. After the modeling was completed, the mice in each group were anesthetized, shaved, and disinfected. All animal experiments were approved by the Animal Care and Use Committee of Shanghai University

of Traditional Chinese Medicine (Shanghai, China) and were performed in accordance with the Ethical Guidelines for the Care and Use of Laboratory Animals.

2.3. HNK treatment

For the evaluation of HNK treatment on alleviation of DDC diet induced chronic cholestasis liver injury, we designed two experiment based on the chronic cholestasis liver injury model.

In the first experiment for the evaluation of the dosage-dependent hepatoprotective effect of HNK, four groups included a negative treated normal control group (NTC group), a negative treated DDC diet fed induced chronic cholestasis liver injury model group (DDC group), two dosages (2 mg/kg, and 10 mg/kg) of HNK treated chronic cholestasis liver injury group (HNK group). DDC diet was daily fed from day 1 to day 28 and HNK was daily intraperitoneal injected from day 15 to day 28. Mice were monitored daily and the body weight was recorded. After 4 weeks of DDC diet fed and responsible HNK treatment for 2 weeks, animals were anesthetized then with pentobarbital (50 mg/kg, intraperitoneal injection) and blood was collected via orbit. Then the abdominal cavity was opened, the liver was removed and weight. The liver was then rinsed with physiological saline. Left lobe and median lobes were separated and put into liquid nitrogen and stored at − 80 °C in ultra-low temperature refrigerator. Sections of the right lobe were fixed and stored in 4% paraformaldehyde overnight at 4 °C for paraffin sectioning.

In the second experiment for the analysis of hepatotoxicity and exploration of the inflammatory regulation of HNK treatment, four groups of mice included a negative treated normal control group (NTC), a high dosage of 10 mg/kg HNK treated normal control group (HNK), a DDC diet fed induced chronic cholestasis liver injury model group (DDC), and high dosage of 10 mg/kg HNK treated chronic cholestasis liver injury group (DDC + HNK). DDC diet was daily fed from day 1 to day 28 and HNK was daily intraperitoneal injected from day 15 to day 28. Mice were then monitored daily and the body weight were recorded. Then mice were anesthetized and EDTA treated blood was collected for flow cytometry analysis. After the liver was removed and weight, fresh livers were rinsed in PBS, the left lobe was used for single cell suspension preparation and flow cytometry analysis, median lobes were put into liquid nitrogen, and the right lobe was fixed in 4% paraformaldehyde for histopathological analysis.

2.4. Serum biochemistry

Blood samples were centrifuged to collect serum. Serum alanine aminotransferase (ALT) and serum aspartate aminotransferase (AST), and alkaline phosphatase (ALP) were measured using an automatic biochemical analyzer with commercial kits (Nanjing Jiancheng Bioengineering Institute, Nanjing, China). The concentrations of total BAs (TBA), total bilirubin (TBIL), and direct bilirubin (DBIL) in serum samples were analyzed by standard enzymatic assays using commercial kits (Nanjing Jiancheng Bioengineering Institute, Nanjing, China). Hepatic BAs were extracted from liver samples using 90% methanol and hepatic BAs were measured using a commercial assay kit (MAK309, Sigma–Aldrich, USA) as previously described.

2.5. Measurement of hepatic collagen content

Hepatic collagen deposition was determined biochemically by measuring the hydroxyproline content with modified method. In short, 500 mg liver samples underwent complete acid hydrolysis in 5 ml of 6 N hydrochloric acid solution at 110 °C for 16 h. After centrifugation at 2000 rpm for 5 min, 2 ml of supernatant was collected and neutralized with 8 N potassium hydroxide solution to pH 6–6.5 and was oxidized with 1 ml of 0.6 mol/l chloramine-T for 30 min. After oxidization, 1 ml of 7.5% p-dimethylaminobenzaldehyde was added and the mixture was incubated for 15 min at 65 °C. Absorbance was measured at 560 nm. Tissue content of hydroxyproline was determined using a standard curve generated from pure hydroxyproline. Results are expressed as μg/g of wet liver tissue. then hydroxyproline was quantitated photometrically as described.

2.6. Histopathology

The live tissue was fixed in 4% paraformaldehyde for at least 24 h and then was subjected to dehydration and penetration. The specimen was then embedded in paraffin. The section was cut at a thickness of 4 μm for haematoxylin and eosin (H&E) staining and Masson's trichrome staining. Pathological changes were observed by light microscopy.

2.7. Immunohistochemistry

The prepared sections (4 μm) were heated at 60 °C for 1 h and then rehydrated with xylene and different concentrations of alcohol. The sections were washed three times with phosphate buffer solution (PBS) to block non-specific binding sites, immersed in 5% bovine serum albumin (BSA) for 20 min at 37 °C and then incubated for 10 min. Specimens were incubated overnight at 4 °C with primary antibodies including CK19 (1:200), CD11b (1:200) and CD3 (1:100). On the second day, after incubation with an appropriate secondary antibody for 30 min at 37 °C, the sections were analysed with a diaminobenzidine kit to detect antibody binding. Finally, the slices were viewed on an ECLIPSE-Ci microscope (Nikon, Japan) and pictures were recorded using a digital camera Pannoramic MIDI II (3DHISTECH, Hungary) or Nano Zoomer S60 (HAMAMATSU, Japan).

2.8. BAs analysis

For serum and hepatic BAs measurements, The BAs concentration of all samples was measured by colorimetric analysis using commercial kit MAK309 (Sigma–Aldrich, USA) according to the manufacturer's instructions. For the exaction of hepatic BAs, 200 mg of liver was homogenized in 1.0 ml of 70% ethanol, shaking incubated at 50 °C for 2 h and centrifuged at 15000 rpm for 15 min.

2.9. Analysis of individual bile acid composition by mass spectrometry

The profiles of individual BAs in biological samples were determined by liquid chromatography tandem mass spectrom-

etry (LC-MS/MS) referencing previous studies (Li et al., 2019, Xue et al., 2021). For sample preparation, a volume of 180 µl of ice-cold alkaline acetonitrile (5% NH_4OH in acetonitrile) was added to 20 µl of biological sample, vortexed, and centrifuged at 15000 rpm for 30 min at 4 °C. The supernatant was aspirated, evaporated under vacuum, and reconstituted in 40 µl of 50% acetonitrile. A volume of 10 µl supernatant was injected into the LC-MS/MS system for quantitative analysis. The instrument conditions were as follows: UHPLC- Q/Exactive mass spectrometer (Thermo Scientific, USA) with Column Hypersil Gold Dim (100 × 2.1 mm, 1.9 µm, USA). Mobile phase A was acetonitrile mobile and phase B was 5 mM ammonium formate with 0.1% formic acid in water. The flow rate was 0.3 ml/min and the gradient was set as, 0–2 min, 5% A–30% A; 2–5 min, 30% A–55% A; 5–16 min, 55% A–95% A; 16–18 min, 95% A; 18–20 min, 95% A–5% A. The mass spectrometer was equipped with an electrospray ionization source. All the BAs were detected in negative ion mode. Multiple reaction monitoring transitions of BAs and internal standard are listed in Supplementary Material of Table S1.

2.10. Quantitative real-time PCR

RNA from the liver was isolated using Trizol reagent (Invitrogen, USA) according to the manufacturers' instructions. RNA concentrations were measured using NanoDrop 2000c spectrophotometer (Thermo Scientific, USA). Total liver RNA (2 µg) was reverse-transcribed into cDNA using Super Script II Reverse Transcriptase (Invitrogen, USA) and the oligo dT method. qPCR was performed using the Stepone Plus System (Applied Biosystems, USA) with SYBR green reagent (TaKaRaBio, Japan), according to manufacturers' instructions. The ΔΔCT method was utilized to assess mRNA expression relative to that of GAPDH, which was used as an internal reference. The primers used for this study are listed in Supplementary Material Table S2.

2.11. Liver perfusion and cell separation

Fresh livers of left lobe were weight, then 500 mg liver tissue was perfused with 0.28 mg/mL collagenase IV (Sigma; C-5138) through the inferior vena cava. The dissociated cells were passed through a 70 mm cell strainer to remove clumps and undigested tissue. Cells were centrifuged mildly at 10 g for 5 min to pellet down hepatocytes and supernatant cells were collected by centrifugation at 350 g for 10 min. Cells were resuspended in 90 ml of running buffer (PBS pH 7.2, 0.5% BSA, and 2 mM EDTA) per 10^7 cells, Erythrocytes were lysed with ACK Lysing Buffer (Thermofisher, USA). Remaining liver cells were suspended in the culture medium for Flow cytometry analysis.

2.12. Flow cytometry

Isolated single cell suspensions were prepared for flow cytometric analysis. Briefly, 5 million cells were incubated with a cocktail of fluorescent conjugated antibodies that summarized in Supplementary Material Table S3. Each incubation step was performed at 4 °C for 30 min and cells were subsequently washed two times in FACS buffer that PBS supplemented 1% fetal calf serum, 2.5 mM EDTA and 0.1% sodium azide. Prior to acquisition, labeled cells were incubated for 1 min with DAPI (Thermofisher, USA) at the final concentration of 1 mg/ml and washed with FACS buffer. Flow cytometric analysis was performed on a CytoFLEX flow cytometer (Beckman Coulter, USA) and analyzed using FlowJo software (TreeStar, Olten, Switzerland). Debris was excluded based on physical parameters (forward and side scatter characteristics, respectively).

2.13. Statistical analysis

All data were collected and analyzed with GraphPad Prism Software version 9.0 for Windows (GraphPad, USA). The data are presented graphically as mean values ± standard deviation (SD). Data significance was compared by the one-way or two-way ANOVA method, followed by Tukey's multiple comparisons test. Statistically significant differences were marked as values of *p < 0.05, **p < 0.01, ***p < 0 0.001, and ***p < 0 0.0001.

3. Results

3.1. HNK attenuated DDC-induced ductular proliferation

We first established a chronic cholestasis liver injury model. DDC feed mice were reported as a successful chronic cholestasis liver injury model in a dose- and time-dependent manner (Pose et al., 2019, Li et al., 2021). In most cases, primary damage to the biliary epithelium leads to the development of cholestasis (Beretta-Piccoli et al., 2019). Long-standing cholestasis causes an ordered bile duct proliferation or typical ductular reaction (Mariotti et al., 2019). In our experiment, a 0.1% DDC containing diet was feed into C57BL/6J mice for 4 weeks showed the hepatomegaly and body weight loss. The significant decreasing body weight and the increasing liver weight were accompanied by the increasing of liver/body weight ratio from 6.1% to 12.9% (Fig. 1A). Macroscopic analysis of the livers of DDC feed mice showed a brownish colour change and hepatomegaly, indicating cholestasis and liver injury. In line with these macroscopic results, the serological analysis also revealed liver injury and cholestasis (Fig. 1B), as shown by significantly increased levels of AST, ALT, and ALP. To evaluate chronic cholestatic liver injury changes of DDC diet, we performed a pathological analysis of livers. The histopathology results of HE staining, masson staining and CK19 immunochemistry of the liver sections showed the typical ductular reaction (Fig. 1C). The ductular reaction was reported to emerge and originate from proliferation of pre-existing bile duct epithelial cells(Mariotti et al., 2019, Pose et al., 2019). Moreover, DDC induced obvious hepatic concentric periductal fibrosis (a typical feature of human cholangitis) that is characterized as chronic obstruction of the biliary tree, accumulation of extracellular matrix at portal tracts, surrounding newly formed bile ducts.

To evaluate the hepatoprotective effect of HNK after referencing the previous studies(Sulakhiya et al., 2015, Elfeky et al., 2020), we used two dosages of HNK (2 mg/kg/day and 10 mg/kg/day) for the treatment of chronic cholestasis liver injury. It was found the hepatomegaly and body weight loss was reversed by the HNK treatment in a dose dependent manner, as well as the elevation of liver/body weight ratio. Moreover,

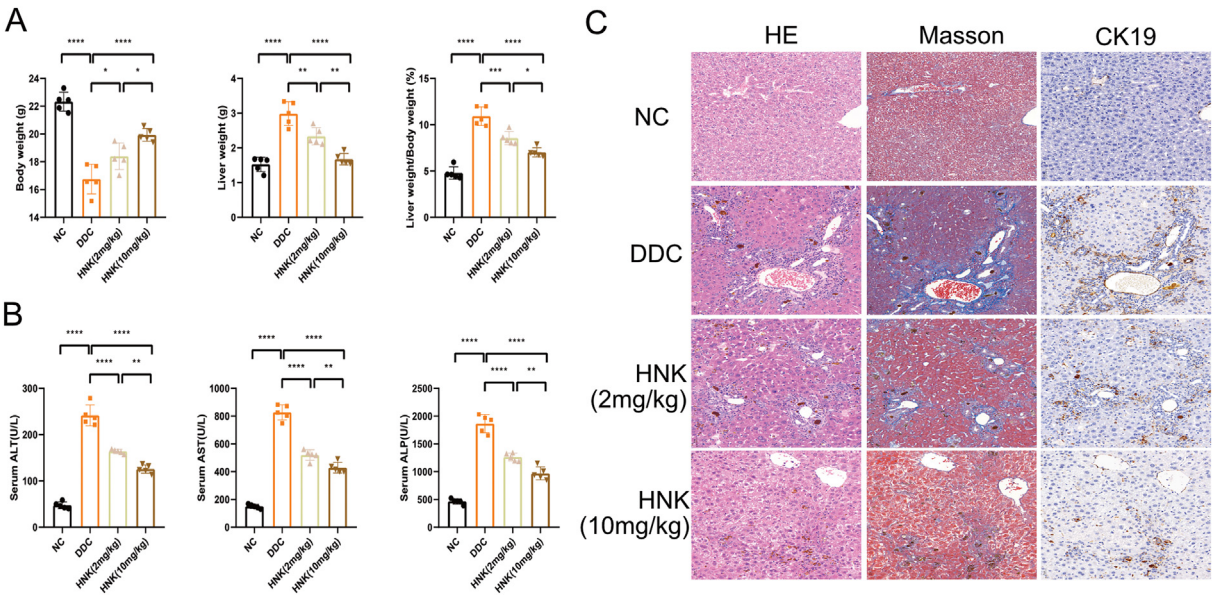

Fig. 1 HNK attenuated DDC-induced ductular proliferation. According to the description in the materials and methods, C57BL/6J mice were fed with DDC diet or treated with different dosages of HNK. (A) The body weight, liver weight, and liver weight to body weight percentage in the DDC diet and HNK treatment groups. (B) The serum levels of ALT, AST, and ALP in the DDC diet and HNK treatment groups. (C) Representative images of hepatic HE staining, Masson staining and immunohistochemistry for CK19 were shown in the DDC diet and HNK treatment groups. The data were presented graphically as mean ± SD and compared by the one-way ANOVA method, followed by Tukey's multiple comparisons test. Five mice for each group from the first in vivo experiment. Significant differences were marked as $*p < 0.05$, $**p < 0.01$, $***p < 0\ 0.001$, and $****p < 0\ 0.0001$.

the increased levels of serological ALT, AST and ALP were relieved. The pathological analysis of livers revealed the hepatoprotective effect of HNK even though typical ductular reaction, fibrosis and infiltration of inflammatory cells around the portal area were alleviated in the two dosages of HNK treatment groups.

3.2. HNK attenuated DDC-induced BAs accumulation

DDC diet feed in mice often induced hepatic accumulation of bilirubin and BAs concentration(Li et al., 2021). The significant elevation of serum total bilirubin and direct bilirubin were observed in DDC diet feed mice with chronic cholestasis liver injury (Fig. 2A). HNK alleviated the elevation of serum total bilirubin and direct bilirubin. Moreover, DDC induced significant increasing of serum and hepatic BAs levels. HNK treatment resulted in dosage-dependent decreasing of serum and hepatic BAs accumulation (Fig. 2B). BAs included a large family of molecules with steroidal structure that synthesized from cholesterol in the liver(Matz-Soja 2020). BAs are physiological detergents that facilitate excretion, absorption, and transport of fats and sterols in the liver. Recent studies showed they modulate bile flow, lipid secretion, key enzymes that involved in overall metabolic homeostasis(Fuchs and Trauner 2022). However, BAs have potent toxic properties for initiating and perpetuating bile duct injury(Ahmadi et al., 2021, Dotan et al., 2022), we then measured primary and secondary BAs. It was found DDC induced CA, β-MCA, TCA, T-α-MCA, T-β-MCA and TCDCA significant increase in hepatic tissue (Fig. 2C). 2 mg/kg HNK countered the elevation of TCA, T-α-MCA, and TCDCA, while 10 mg/kg HNK reversed the elevation of β-MCA, TCA, T-α-MCA, T-β-MCA and TCDCA. Furthermore, the secondary BAs, such as ω-MCA, TDCA, TUDCA and T-ω-MCA were also increased after DDC feed for 4 weeks, and HNK countered all the four elevation secondary BAs (Fig. 2D). These results indicated HNK attenuated DDC induced hepatic BAs accumulation and alleviated BAs mediated cytotoxicity in the liver.

The hepatotoxicity of DDC feed mice were also reflected by the significant increasing of hepatic CK19 gene expression (Fig. 2E). It was lined with the liver immunohistochemical results of CK19. HNK treatment resulted in decreasing expression of hepatic CK19 gene expression. Based on the toxic BAs hypothesis (Woolbright and Jaeschke 2019), we further measured the gene expression of enzyme responsible for BAs synthesis. It was found the two enzymes of *Cyp7a1* and *Cyp8b1*, were significant decrease after DDC feed, as previous study (Wen et al., 2021) (Fig. 2F). These enzymes were involved in the classical pathway of BAs synthesis(Fuchs and Trauner 2022). HNK alleviated the inhibition of these two enzymes and implied HNK reprogramed the synthesis of hepatic BAs. Moreover, the alternative pathway of BAs synthesis genes *Cyp27a1* and *Cyp7b1* were inhibited by DDC diet feed (Fig. 2G). HNK showed dosage-dependent increase of *Cyp27a1* and *Cyp7b1* genes expression found a significant reduction of BAs concentration after HNK treatment. indicating HNK was partly beneficial to the excretion of BAs and maintenance of BAs homeostasis. The relationships between the hepatobiliary-protective effect of HNK and BAs regulation was described for the first time. It was reported that HNK can evidently relieve hepatocyte injuries and help to promote the secretion of BAs and benefit the jaundice.

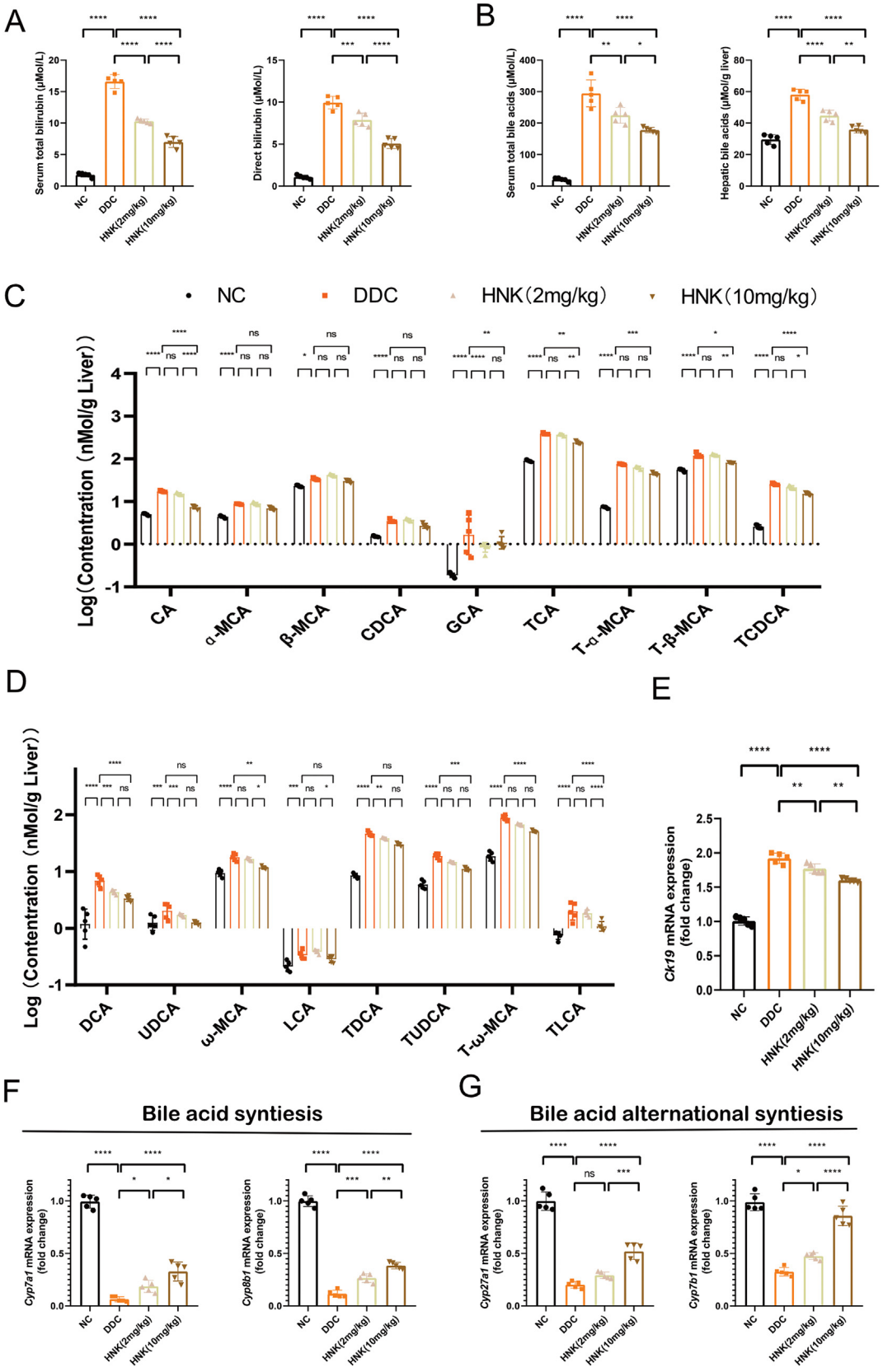
A
Serum total bilirubin (μMol/L)
Direct bilirubin (μMol/L)
B
Serum total bile acids (μMol/L)
Hepatic bile acids (μMol/g liver)
NC
DDC
HNK(2mg/kg)
HNK(10mg/kg)
C
Log (Contentration (nMol/g Liver))
CA
α-MCA
β-MCA
CDCA
GCA
TCA
T-α-MCA
T-β-MCA
TCDCA
D
Log (Contentration (nMol/g Liver))
DCA
UDCA
ω-MCA
LCA
TDCA
TUDCA
T-ω-MCA
TLCA
E
Ck19 mRNA expression (fold change)
F
Bile acid syntiesis
Cyp7a1 mRNA expression (fold change)
Cyp8b1 mRNA expression (fold change)
G
Bile acid alternational syntiesis
Cyp27a1 mRNA expression (fold change)
Cyp7b1 mRNA expression (fold change)

3.3. HNK alleviated DDC-induced BAs metabolism, uptake, efflux, and transporter

Since hepatic BAs were elevated and these BAs had potential toxic properties of membrane disruption(Woolbright and Jaeschke 2019). At present, novel therapeutic approaches for the treatment of cholestatic liver diseases focused on the metabolism and circulation of BAs(Fuchs and Trauner 2022). We then investigated the effect of HNK on the BAs regulation, including metabolism, efflux, intake and circulation. It was consistent with previous research results (Fickert et al., 2007) that DDC induced gene expression elevation of phase I metabolism enzyme of *Cyp3a11* and *Cyp2b10* (Fig. 3A), as well as phase II metabolism enzymes of *Sult2a1* and *Ugt1a1* (Fig. 3B). These activation of BAs metabolism was mainly resulted in the high BAs. HNK treatment groups showed moderate arise of the genes expression that were responsible for BAs phase I and II metabolism. BAs recirculate through the liver, bile ducts, small intestine and portal vein to form an enterohepatic circuit (St-Pierre et al., 2001). DDC induced decreasing genes expression of *Ntcp* and *Oatp1*(Fig. 3C). These two genes responsible for the uptake of BAs into hepatocytes. The high levels of hepatic BAs impaired the uptake of BAs into hepatocytes. The BAs efflux into bile were also blocked since the genes expression of *Bsep* and *Mrp2* was decreasing (Fig. 3D). It was interesting HNK treatment alleviated BAs uptake into hepatocytes and efflux into bile. High dosage of 10 mg/kg HNK showed a significant stronger activation of *Ntcp, Oatp1, Bsep* and *Mrp2* than low dosage of 2 HNK. The accumulated hepatic BAs efflux into systemic circulation through canalicular export pumps of *Osta, Ostb, Mrp3* and *Mrp4*, thus resulted in the accumulation of BAs in the serum. Our results showed DDC diet induced decreasing expression of *Osta, Ostb,* and *Mrp3* (Fig. 3E). HNK treatment encountered the BAs alternative basolateral efflux pumps. Taken together, HNK partially recovered the BAs transporters and the bile flow was consistent with the relatively moderate cholestasis liver injury.

3.4. HNK attenuated DDC-induced inflammatory response

Previous HE staining results showed obvious infiltration of inflammatory cells surrounding newly formed bile ducts (Fig. 1C). We thus performed immunohistochemically analysis of liver infiltrating inflammatory cells based on staining of CD11b and CD3. CD11b was mainly expressed on the surface of myeloid cells including monocytes, macrophages and Kupffer cells. Functionally, CD11b regulates myeloid cells adhesion and migration to the injured live and mediate the inflammatory response for the hepatoprotective effect. We found a diffuse high expression of CD11b positive cells in the liver of DDC feed mice (Fig. 4A). HNK treatment resulted in moderate infiltration of myeloid cells in the liver. CD3 positive lymphocytes were also aggregated and surrounded the newly formed bile ducts. HNK treatment group showed a decreasing infiltration of CD3 positive cells in the DDC induced cholestasis-related liver. Mcp-1 was an important chemokine that regulates migration and infiltration of monocytes and macrophages. Previous studies also showed the increasing of *Mcp-1* in the DDC induced cholestasis-related liver(Wen et al., 2021). We verified the increased *Mcp-1* gene expression in the DDC group (Fig. 4B). The descending *Mcp-1* expression in the HNK treatment groups indicated its inhibition of infiltration of inflammatory cells in the cholestasis-related liver. The cytokines of *Tnf-a, Il-1β,* and *Il-6* were not only associated with inflammatory cells, but also played multiple effects on ductular reactions and fibrosis(Pose et al., 2019). We then measured the gene expression of inflammatory related cytokines in the liver. DDC diet feed group showed abnormally elevation of *Tnf-α, Il-1β,* and *Il-6* (Fig. 4C). HNK treatment alleviated the elevation of classical cytokines of *Tnf-a, Il-1β,* and *Il-6*. During this inflammatory response, inflammatory cells also release TGF-β1 to enhance their protein synthesis and metabolic activity(Gough et al., 2021). Among the pro-inflammatory and pro-fibrotic properties, Tgfb1 stimulate recruitment, proliferation and activation of a various of cells, especially fibroblasts for the deposition of extracellular matrix and stabilize the fibrotic tissue architecture. We confirmed the elevation of *Tgfb1* gene expression in the DDC feed group (Wen et al., 2021) (Fig. 4D). HNK treatment showed a dosage-dependent alleviation of elevating *Tgfb1* and indicated the consistent inhibition of fibrosis phenotypes.

3.5. HNK alleviated DDC-induced infiltration of inflammatory cells

Previous studies revealed the decreasing of Kupffer cells and increasing of monocyte derived macrophages in the DDC induced cholestasis-related liver(Gough et al., 2021). Lymphocytes were also investigated for the development of DDC induced cholestasis liver injury(Fickert et al., 2007). To analysis the infiltration of inflammatory cells and reveal the hepatotoxicity of high dosage of HNK, we designed dependent experiment of high dosage of HNK (10 mg/kg/day) for 28 days continuously treatment for the control group and DDC diet feed groups. It was consistent with previous study that DDC induced hepatomegaly and weight loss were reversed by HNK treatment (Fig. 5A). It was noted HNK treatment in control mice showed no significant difference of body weight and liver weight. The peripheral blood mononuclear cells and hepatic single cells suspension were prepared for flow

Fig. 2 HNK attenuated DDC-induced bile acids accumulation. (A) The serum total bilirubin and direct bilirubin concentrations in the DDC diet and HNK treatment groups. (B) The serum bile acid and hepatic bile acid levels in the DDC diet and HNK treatment groups. (C) The hepatic individual primary bile acid levels in the DDC diet and HNK treatment groups. (D)The hepatic individual secondary bile acid levels in the DDC diet and HNK treatment groups. (E) The hepatic gene expression of Ck19 in the DDC diet and HNK treatment groups. (F) The hepatic gene expression of *Cyp7a1* and *Cyp8b1* in the DDC diet and HNK treatment groups. (G) The hepatic gene expression of *Cyp27a1* and *Cyp7b1* in the DDC diet and HNK treatment groups. The data were presented graphically as mean ± SD and compared by the one-way or two-way ANOVA method, followed by Tukey's multiple comparisons test. Five mice for each group from the first in vivo experiment. Significant differences were marked as $*p < 0.05$, $**p < 0.01$, $***p < 0\ 0.001$, and $****p < 0\ 0.0001$.

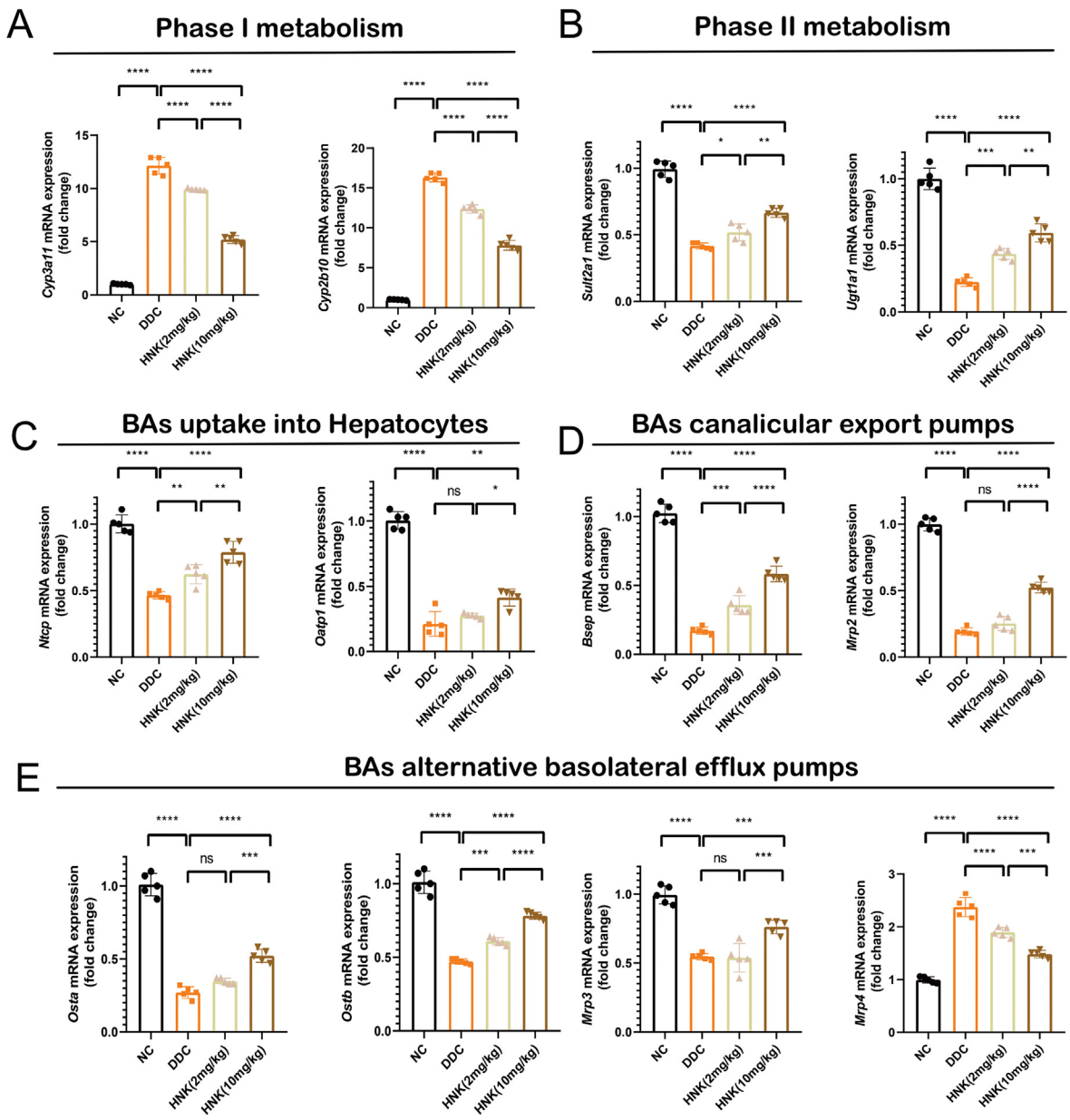

Fig. 3 HNK alleviated DDC-induced bile acids metabolism, uptake, efflux, and transporter. (A) The hepatic gene expression of *Cyp3a11* and *Cyp2b10* in the DDC diet and HNK treatment groups. (B) The hepatic gene expression of *Sult2a1* and *Ugt1a1* in the DDC diet and HNK treatment groups. (C) The hepatic gene expression of *Ntcp* and *Oatp1* in the DDC diet and HNK treatment groups. (D) The hepatic gene expression of *Bsep* and *Mrp2* in the DDC diet and HNK treatment groups. (E) The hepatic gene expression of *Osta, Ostb, Mrp3* and *Mrp4* in the DDC diet and HNK treatment groups. The data were presented graphically as mean ± SD and compared by the one-way ANOVA method, followed by Tukey's multiple comparisons test. Five mice for each group from the first in vivo experiment. Significant differences were marked as $*p < 0.05$, $**p < 0.01$, $***p < 0\ 0.001$, and $****p < 0\ 0.0001$.

cytometry. An optimized flow cytometry strategy for the simultaneous analysis of hepatic lymphoid cells and myeloid cells were developed based on literature(Liu et al., 2020, Cossarizza et al., 2021) (Fig. 5B). It was found there was a significant increase of leukocytes based on liver CD45 + cells in the DDC induced cholestasis-related liver (Fig. 5C). HNK treatment group showed a descending infiltration of leukocytes when compared with DDC diet induced cholestasis liver injury groups. However, there was no significant difference of infiltrating leukocytes when compared HNK treated control mice when compared with NTC group. For the analysis of myeloid cells of CD11b + cells, we further separated monocyte derived macrophages and kupffer cells. It was found DDC induced increasing infiltration of monocyte derived macrophages (MoDMacs) (Fig. 5D). However, the Kupffer cells was depleted after DDC diet feed. HNK treatment in DDC diet feed mice not only increased the infiltrated MoDMacs percentage, but also preserved the depletion of Kupffer cells when compared with DDC diet feed mice. For the lymphoid cells, we first distinct CD3 + lymphocytes, and found there was a significant increasing of infiltrating CD3 + T lymphocytes after DDC feed, and a moderate decline of CD3 + T lympho-

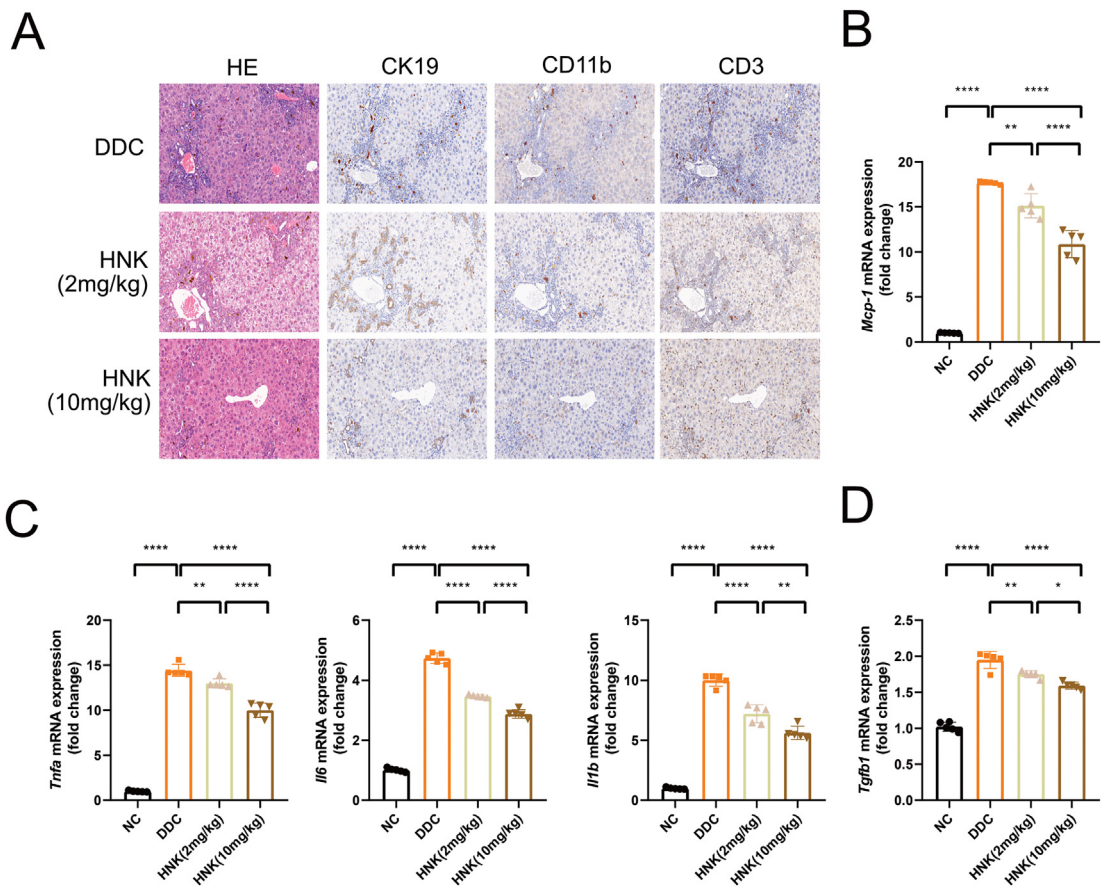

Fig. 4 HNK attenuated DDC-induced inflammatory response. (A) Representative images of hepatic HE staining and immunohistochemistry for CK19, CD11b and CD3 were shown in the DDC diet and HNK treatment groups. (B) The hepatic gene expression of *Mcp-1* in the DDC diet and HNK treatment groups. (C) The hepatic gene expression of *Tnfa, Il6,* and *Il1b* in the DDC diet and HNK treatment groups. (D) The hepatic gene expression of Tgfb1 in the DDC diet and HNK treatment groups. The data were presented graphically as mean ± SD and compared by the one-way ANOVA method, followed by Tukey's multiple comparisons test. Five mice for each group from the second in vivo experiment. Significant differences were marked as *p < 0.05, **p < 0.01, ***p < 0 0.001, and ****p < 0 0.0001.

cytes infiltration after HNK treatment (Fig. 5E). Moreover, CD4 + and CD8 + T lymphocytes were analyzed and we confirmed the significant increasing infiltration of CD8 + T lymphocytes and decreasing infiltration of CD8 + T lymphocytes after DDC diet feed. HNK treatment showed a decreasing of CD8 + T lymphocytes and an alleviation of CD4 + T lymphocytes infiltration in the DDC induced cholestasis-related liver. The infiltration of leukocytes was associated with production and secretion of pro-inflammatory cytokines. Thus we measured the hepatic cytokines of TNF-α, and IL-6 (Fig. 5F). There was significant increasing of cytokines TNF-αand IL-6 after DDC feed, and moderate decreasing of cytokines TNF-α and IL-6 after HNK treatment. These result indicated the DDC induced infiltration of inflammatory cells and production of cytokines were countered by the HNK treatment.

4. Discussion

Chronic cholestasis liver injury is one of the most common and devastating liver diseases. Currently, there is no effective treatment for chronic cholestasis liver injury and patients are at risk of developing end-stage liver disease and multiple organ failure. Studies for the treatment of cholestasis liver disease gradually focus on the regulation of BAs metabolic homeostasis and inflammation response. In the present study, we used the DDC induced chronic cholestasis liver injury model for evaluating the pharmacological effect of HNK from two dependent experiment. HNK displayed a dosage-dependent reduction of ductular reaction, regulation of BAs metabolism and inhibition of inflammatory response. Moreover, there was litter hepatotoxicity since the high dosage of HNK for 28 days' treatment in control mice resulted in no obvious change of hepatic histopathological and serological changes.

Cytotoxic BAs accumulation in liver apparently contributed to the occurrence of ductular reaction. BAs function as intracellular signaling molecules in a variety of cells and change cellular functions such as proliferation, differentiation, apoptosis, liver regeneration, and modulation of metabolic homeostasis(Perino et al., 2021). Specifically, BAs injure biliary epithelial cells and cholangiocyte in mice lacking canalicular phospholipid transporter (Miethke et al., 2016). The increased concentration of BAs in the liver also trigger proliferation of biliary epithelial cells and cholangiocyte in chronic cholestasis (Cai and Boyer 2021). In the present study, DDC

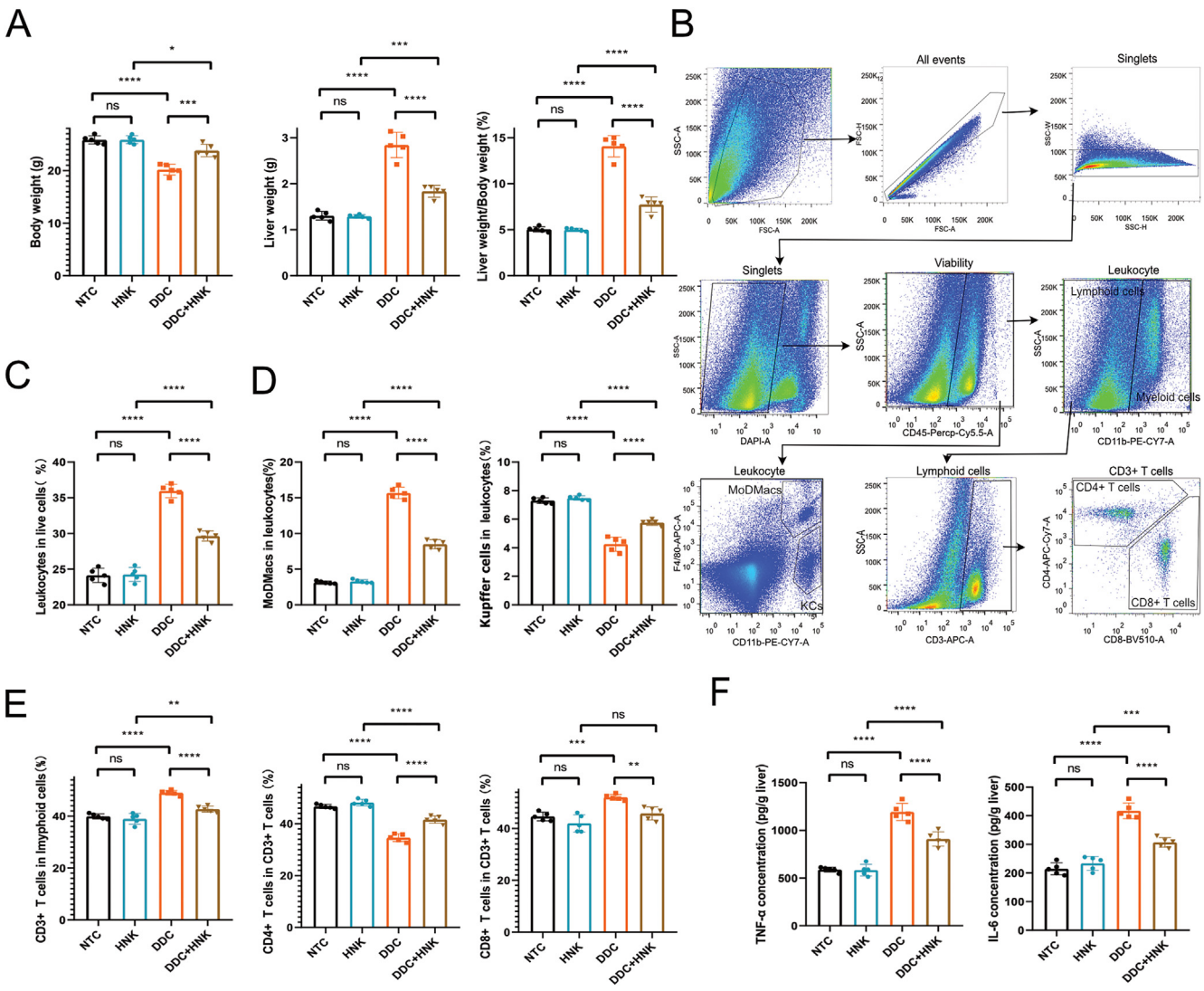

Fig. 5 HNK alleviated DDC-induced infiltration of inflammatory cells. (A) The body weight, liver weight, and liver weight to body weight percentage in the DDC diet and HNK treatment groups. (B) The representative flow cytometry strategy for analyzing the hepatic infiltrating immunocytes. (C) The hepatic leukocyte percentage in the DDC diet and HNK treatment groups. (D) The hepatic MoDMacs and Kupffer cells percentages in the DDC diet and HNK treatment groups. (E) The hepatic CD3 + T cells in lymphoid cells, as well as CD4 + and CD8 + T cells in CD3 + T cells percentages in the DDC diet and HNK treatment groups. (F) The hepatic inflammatory levels of TNF-α and IL-6 in the DDC diet and HNK treatment groups. The data were presented graphically as mean ± SD and compared by the one-way ANOVA method, followed by Tukey's multiple comparisons test. Five mice for each group from the second in vivo experiment. Significant differences were marked as $*p < 0.05$, $**p < 0.01$, $***p < 0\ 0.001$, and $****p < 0\ 0.0001$.

induced chronic cholestasis liver injury was showed atypical ductular reaction around periphery of portal tracts and elevation of hepatic BAs concentration. The labyrinth of ductular reaction was consistent with the increase gene and protein expression of CK19. Moreover, the elevated hepatic BAs inhibited the genes expression of BAs synthesis, and activated the gene expression of BAs phase I metabolism. It was noted the hepatic accumulation of BAs was associated with the reprogramming of BAs transporters. The 28 days' DDC diet feed resulted in decreasing gene expression of *Ntcp, Oatp1, Bsep, Mrp2, Osta, Ostb,* and *Mrp3*, as well as increasing *Mrp4*. HNK treatment showed dosage-dependent moderate inhibition of BAs accumulation. Moreover, HNK reprogramed the BAs synthesis, metabolism, and transporters.

Previous studies have shown that elevated BAs levels induced hepatic inflammation, including infiltration of leukocytes and production of cytokines(Li et al., 2017). Similar with previous reports, we confirmed the increasing infiltration of inflammatory cells and production of cytokines after DDC diet feed(Jiang et al., 2019). HNK showed potent anti-inflammatory response not only featured as attenuation of myeloid and lymphoid cells infiltration, but also characterized as inhibition of cytokine TNF-α and IL-1β production. Furthermore, the chronic cholestasis liver injury of DDC diet feed gradually induced Kupffer cells depletion, and infiltration of MoDMars. Kupffer cells are the most abundant liver resident macrophages for maintaining tissue homeostasis and are involved in various liver diseases(Jemail et al., 2018). In a

chronic liver disease setting, depletion of Kupffer cells were frequently association with massive infiltration of MoDMars and excessive inflammatory responses. HNK ameliorated the inflammatory response through decreasing macrophages population and preserved the Kupffer cells percentage.

HNK is a biphenolic natural compound isolated from the leaves and barks of Magnolia plant species and has been extensively studied for its beneficial effects against several chronic diseases. HNK demonstrated anti-inflammatory and metabolic regulation properties from in vitro and in vivo models. Honokiol targets multiple inflammatory signaling and metabolism pathways including nuclear factor kappa B (NF-κB), signal transducers and activator of transcription 3 (STAT3), and mammalian target of rapamycin (m-TOR). To date, pharmacological treatments of HNK as herbal therapy on chronic liver injury became popular for their clinical efficacy with minimal side effects. We found NHK exert dosage-dependent of pharmacological effect against DDC induced chronic cholestasis liver injury. Moreover, the high dosage of HNK treatment for 28 days showed no obvious hepatotoxicity. The antifibrosis effect of HNK was observed from histopathological changes of Masson staining, that was consistent with previous studies (Cao et al., 2005, Elfeky et al., 2020, Lee et al., 2021). Further preclinical research about pharmacological effect and mechanism of HNK against chronic cholestasis liver injury is needed for the drug development.

5. Conclusion

In summary, HNK displayed a dosage-dependent hepatic protective effect against DDC induced chronic cholestasis liver injury that featured as alleviation of ductular reaction, BAs accumulation, fibrosis and inflammatory response. The mechanism of HNK mainly focused on the regulation of BAs metabolism, decrease of inflammatory cell infiltration and inhibition of pro-inflammatory cytokines production. Moreover, HNK showed no hepatotoxicity even with the high dosage of HNK for 28 days' treatment. All these results elucidated the potent hepatpprotective effect of HNK against chronic cholestasis liver disease.

CRediT authorship contribution statement

Juan Hao: . **Xiaoyu Shen:** . **Xiaohong Shao:** . **Chunling Zhu:** . **Kan Lu:** . **Yi Xu:** . **Yiyue Chen:** . **Jibo Liu:** . **Yaqin Ding:** . **Xin Xie:** Resources. **Jian Wu:** Resources, Conceptualization. **Quanjun Yang:** Resources, Conceptualization.

Declaration of Competing Interest

The authors declare that they have no known competing financial interests or personal relationships that could have appeared to influence the work reported in this paper.

Acknowledgements

This study was supported by grants from the National Natural Science Foundation of China (No.: 81803874, J.H.), Shanghai Pujiang Talent Program (China, No.: 21PJ1411900, Q.Y.), Shanghai Three-Year Action Plan of Specialty Cultivation and Promotion Project (China, No.: HGY-YSZK-2018-13, J. W.), Clinical Medicine Outstanding Young Talents of HongKou (China, No.: HKYQ2017-24, J.W.), HongKou District Health Committee Project (China, No.: HKQ-ZYY-2021-12, X.X.), and Project of Shanghai TCM-Integrated Hospital (China, No.: RCPY0028, Y.X.).

Appendix A. Supplementary material

Supplementary data to this article can be found online at https://doi.org/10.1016/j.arabjc.2023.104968.

References

Ahmadi, A., Niknahad, H., Li, H., et al, 2021. The inhibition of NFκB signaling and inflammatory response as a strategy for blunting bile acid-induced hepatic and renal toxicity. Toxicol. Lett. 349, 12–29.

Beretta-Piccoli, B.T., Mieli-Vergani, G., Vergani, D., et al, 2019. The challenges of primary biliary cholangitis: What is new and what needs to be done. J. Autoimmun. 105, 102328.

Cai, S.Y., Boyer, J.L., 2021. The role of bile acids in cholestatic liver injury. Ann. Translat. Med. 9, 737. https://doi.org/10.21037/atm-20-5110.

Cao, A.H., Vo, L.T., King, R.G., 2005. Honokiol protects against carbon tetrachloride induced liver damage in the rat. Phytother. Res.: Int. J. Devoted Pharmacol. Toxicol. Eval. Nat. Prod. Derivatives 19, 932–937.

Chen, G., Izzo, J., Demizu, Y., et al, 2009. Different redox states in malignant and nonmalignant esophageal epithelial cells and differential cytotoxic responses to bile acid and honokiol. Antioxid. Redox Signal. 11, 1083–1095.

Cossarizza, A., Chang, H.D., Radbruch, A., et al, 2021. Guidelines for the use of flow cytometry and cell sorting in immunological studies. Eur. J. Immunol. 51, 2708–3145. https://doi.org/10.1002/eji.202170126.

Dotan, M., Fried, S., Har-Zahav, A., et al, 2022. Periductal bile acid exposure causes cholangiocyte injury and fibrosis. PLoS One 17, e0265418.

Elfeky, M.G., Mantawy, E.M., Gad, A.M., et al, 2020. Mechanistic aspects of antifibrotic effects of honokiol in Con A-induced liver fibrosis in rats: emphasis on TGF-beta/SMAD/MAPK signaling pathways. Life Sci. 240,. https://doi.org/10.1016/j.lfs.2019.117096 117096.

Fickert, P., Stoger, U., Fuchsbichler, A., et al, 2007. A new xenobiotic-induced mouse model of sclerosing cholangitis and biliary fibrosis. Am. J. Pathol. 171, 525–536. https://doi.org/10.2353/ajpath.2007.061133.

Fuchs, C.D., Trauner, M., 2022. Role of bile acids and their receptors in gastrointestinal and hepatic pathophysiology. Nat. Rev. Gastroenterol. Hepatol., 1–19

Gough, N.R., Xiang, X., Mishra, L., 2021. TGF-β signaling in liver, pancreas, and gastrointestinal diseases and cancer. Gastroenterology 161 (434–452), e415.

Ibrahim, S.H., Kamath, B.M., Loomes, K.M., et al, 2022. Cholestatic liver diseases of genetic etiology: advances and controversies. Hepatology 75, 1627–1646. https://doi.org/10.1002/hep.32437.

Jemail, L., Miyao, M., Kotani, H., et al, 2018. Pivotal roles of Kupffer cells in the progression and regression of DDC-induced chronic cholangiopathy. Scient. Rep. 8, 6415. https://doi.org/10.1038/s41598-018-24825-x.

Jeong, H.-U., Kim, J.-H., Kong, T.Y., et al, 2016. Comparative metabolism of honokiol in mouse, rat, dog, monkey, and human hepatocytes. Arch. Pharm. Res. 39, 516–530.

Jiang, A., Okabe, H., Popovic, B., et al, 2019. Loss of Wnt secretion by macrophages promotes hepatobiliary injury after administration of 3,5-Diethoxycarbonyl-1, 4-Dihydrocollidine diet. Am. J. Pathol. 189, 590–603. https://doi.org/10.1016/j.ajpath.2018.11.010.

Jiraviriyakul, A., Songjang, W., Kaewthet, P., et al, 2019. Honokiol-enhanced cytotoxic T lymphocyte activity against cholangiocarci-

noma cells mediated by dendritic cells pulsed with damage-associated molecular patterns. World J. Gastroenterol. 25, 3941.
Kim, B.H., Cho, J.Y., 2008. Anti-inflammatory effect of honokiol is mediated by PI3K/Akt pathway suppression 1. Acta Pharmacol. Sin. 29, 113–122.
Kim, Y.J., Choi, M.S., Cha, B.Y., et al, 2013. Long-term supplementation of honokiol and magnolol ameliorates body fat accumulation, insulin resistance, and adipose inflammation in high-fat fed mice. Mol. Nutr. Food Res. 57, 1988–1998.
Lee, S.-Y., Cho, J.-Y., 2009. Inhibitory effects of honokiol on LPS and PMA-induced cellular responses of macrophages and monocytes. BMB Rep. 42, 574–579.
Lee, I.H., Im, E., Lee, H.J., et al, 2021. Apoptotic and antihepatofibrotic effect of honokiol via activation of GSK3β and suppression of Wnt/β-catenin pathway in hepatic stellate cells. Phytother. Res. 35, 452–462.
Lee, J.-H., Jung, J.Y., Jang, E.J., et al, 2015. Combination of honokiol and magnolol inhibits hepatic steatosis through AMPK-SREBP-1 c pathway. Exp. Biol. Med. 240, 508–518.
Li, M., Cai, S.-Y., Boyer, J.L., 2017. Mechanisms of bile acid mediated inflammation in the liver. Mol. Aspects Med. 56, 45–53.
Li, W.K., Wang, G.F., Wang, T.M., et al, 2019. Protective effect of herbal medicine Huangqi decoction against chronic cholestatic liver injury by inhibiting bile acid-stimulated inflammation in DDC-induced mice. Phytomed. : Int. J. Phytother. Phytopharmacol. 62,. https://doi.org/10.1016/j.phymed.2019.152948 152948.
Li, Y., Xue, H., Fang, S., et al, 2021. Time-series metabolomics insights into the progressive characteristics of 3,5-diethoxycarbonyl-1,4-dihydrocollidine-induced cholestatic liver fibrosis in mice. J. Pharm. Biomed. Anal. 198,. https://doi.org/10.1016/j.jpba.2021.113986 113986.
Liu, Z., Gu, Y., Shin, A., et al, 2020. Analysis of myeloid cells in mouse tissues with flow cytometry. STAR Protocols 1,. https://doi.org/10.1016/j.xpro.2020.100029 100029.
Ma, X., Jiang, Y., Zhang, W., et al, 2020. Natural products for the prevention and treatment of cholestasis: a review. Phytother. Res. : PTR. 34, 1291–1309. https://doi.org/10.1002/ptr.6621.
Mariotti, V., Cadamuro, M., Spirli, C., et al, 2019. Animal models of cholestasis: an update on inflammatory cholangiopathies. Biochim. Biophys. Acta Mol. Basis Disease 1865, 954–964. https://doi.org/10.1016/j.bbadis.2018.07.025.
Matz-Soja, M., 2020. Bile Acids as Regulatory Signalling Molecules. Springer, Mammalian Sterols, pp. 101–116.
Miethke, A.G., Zhang, W., Simmons, J., et al, 2016. Pharmacological inhibition of apical sodium-dependent bile acid transporter changes bile composition and blocks progression of sclerosing cholangitis in multidrug resistance 2 knockout mice. Hepatology 63, 512–523.
Pablo Arab, J., Cabrera, D., Arrese, M., 2017. Bile acids in cholestasis and its treatment. Ann. Hepatol. 16 (Suppl 1), S53–S57. https://doi.org/10.5604/01.3001.0010.5497.
Park, E.-J., Kim, S.-Y., Zhao, Y.-Z., et al, 2006. Honokiol reduces oxidative stress, c-jun-NH2-termial kinase phosphorylation and protects against glycochenodeoxycholic acid-induced apoptosis in primary cultured rat hepatocytes. Plantamedica 72, 661–664.
Perino, A., Demagny, H., Velazquez-Villegas, L., et al, 2021. Molecular physiology of bile acid signaling in health, disease, and aging. Physiol. Rev. 101, 683–731.
Pose, E., Sancho-Bru, P., Coll, M., 2019. 3,5-Diethoxycarbonyl-1,4-Dihydrocollidine diet: a rodent model in cholestasis research. Methods Mol. Biol. 1981, 249–257. https://doi.org/10.1007/978-1-4939-9420-5_16.
Rajgopal, A., Missler, S.R., Scholten, J.D., 2016. Magnolia officinalis (Hou Po) bark extract stimulates the Nrf2-pathway in hepatocytes and protects against oxidative stress. J. Ethnopharmacol. 193, 657–662.
Seo, M.S., Hong, S.-W., Yeon, S.H., et al, 2014. Magnolia officinalis attenuates free fatty acid-induced lipogenesis via AMPK phosphorylation in hepatocytes. J. Ethnopharmacol. 157, 140–148.
Seo, M.S., Kim, J.H., Kim, H.J., et al, 2015. Honokiol activates the LKB1–AMPK signaling pathway and attenuates the lipid accumulation in hepatocytes. Toxicol. Appl. Pharmacol. 284, 113–124.
Shi, M., Tang, J., Zhang, T., et al, 2022. Swertiamarin, an active iridoid glycoside from Swertia pseudochinensis H. Hara, protects against alpha-naphthylisothiocyanate-induced cholestasis by activating the farnesoid X receptor and bile acid excretion pathway. J. Ethnopharmacol. 291, 115164.
Shi, K., Wen, J., Zeng, J., et al, 2021. Preclinical evidence of Yinchenhao decoction on cholestasis: a systematic review and m eta-analysis of animal studies. Phytother. Res. 35, 138–154.
St-Pierre, M.V., Kullak-Ublick, G.A., Hagenbuch, B., et al, 2001. Transport of bile acids in hepatic and non-hepatic tissues. J. Exp. Biol. 204, 1673–1686. https://doi.org/10.1242/jeb.204.10.1673.
Sulakhiya, K., Kumar, P., Gurjar, S.S., et al, 2015. Beneficial effect of honokiol on lipopolysaccharide induced anxiety-like behavior and liver damage in mice. Pharmacol Biochem Behav. 132, 79–87. https://doi.org/10.1016/j.pbb.2015.02.015.
Wang, R., Cheng, N., Peng, R., et al, 2020. Oral herbal medicine for women with intrahepatic cholestasis in pregnancy: a systematic review of randomized controlled trials. BMC Complement. Med. Therap. 20, 1–24.
Wen, M., Liu, Y., Chen, R., et al, 2021. Geniposide suppresses liver injury in a mouse model of DDC-induced sclerosing cholangitis. Phytother. Res. : PTR. 35, 3799–3811. https://doi.org/10.1002/ptr.7086.
Woolbright, B.L., 2020. Inflammation: cause or consequence of chronic cholestatic liver injury. Food Chem. Toxicol. : Int. J. Published Br. Industrial Biol. Res. Assoc. 137,. https://doi.org/10.1016/j.fct.2020.111133 111133.
Woolbright, B.L., Jaeschke, H., 2012. Novel insight into mechanisms of cholestatic liver injury. World J. Gastroenterol.: WJG 18, 4985.
Woolbright, B.L., Jaeschke, H., 2019. Inflammation and cell death during cholestasis: the evolving role of bile acids. Gene Expr. 19, 215.
Xue, H., Fang, S., Zheng, M., et al, 2021. Da-Huang-Xiao-Shi decoction protects against3, 5-diethoxycarbonyl-1,4-dihydroxychollidine-induced chronic cholestasis by upregulating bile acid metabolic enzymes and efflux transporters. J. Ethnopharmacol. 269,. https://doi.org/10.1016/j.jep.2020.113706 113706.
Yang, F., Wang, Y., Li, G., et al, 2018. Effects of corilagin on alleviating cholestasis via farnesoid X receptor-associated pathways in vitro and in vivo. Br. J. Pharmacol. 175, 810–829.
Yin, H.-Q., Je, Y.-T., Kim, Y.-C., et al, 2009. Magnolia officinalis reverses alcoholic fatty liver by inhibiting the maturation of sterol regulatory element–binding protein-1c. J. Pharmacol. Sci. 109, 486–495.
Yu, F.-L., Wu, J.-W., Zhu, H., 2019. Honokiol alleviates acetaminophen-induced hepatotoxicity via decreasing generation of acetaminophen-protein adducts in liver. Life Sci. 230, 97–103.
YueCheng, Y. and C. ChengWei, 2019. Current status and research interests of the diagnosis and treatment of cholestatic liver disease, 临床肝胆病杂志. 35: 241-246